THE ADIABATIC CLOUD MODEL AS DIAGNOSTIC FOR THE FIRST INDIRECT AEROSOL EFFECT BASED ON MSG SEVIRI AND GROUND OBSERVATIONS

Daniel Merk[1], Hartwig Deneke[1], Bernhard Pospichal[2], Patric Seifert[1], Albert Ansmann[1]

(1) Leibniz Institute for Tropospheric Research, Permoserstraße 15, Leipzig, Germany
(2) University of Leipzig, Stephanstr. 3, 04103 Leipzig, Germany

Abstract

To investigate the first indirect aerosol effect from a satellite perspective, key quantities are the cloud droplet number concentration and the geometrical cloud depth. A retrieval of these quantities requires assumptions about the vertical distribution of the liquid water within the clouds. Therefore adiabatic models have often been used in previous studies. Ground-based remote sensing instruments can be used to shed light on the validity of this adiabatic model. While the geometrical cloud depth can be detected by cloud radar and ceilometer with high accuracy, for the retrieval of cloud droplet number concentration more assumptions are necessary. Herein we apply two approaches to retrieve the cloud droplet number concentration. The first method builds upon existing radar-radiometer retrievals, while the seconds applies an optimal estimation method. Given the optimal estimation of cloud droplet number concentration, we find for a case study at Leipzig that clouds are sub-adiabatic, what is likely caused by entrainment processes.

1. MOTIVATION

The first indirect aerosol effect (Twomey, 1977) remains one of the main uncertainties in projections of anthropogenic climate change. Only with geostationary satellites like MSG we achieve cloud properties with high temporal resolution over a larger area. The retrieval of cloud optical depth and effective radius (reff) is widely applied using a retrieval based on the method described by Nakajima and King (1990). The two cloud key quantities to investigate the first indirect aerosol effect are the cloud droplet number concentration and the cloud geometrical depth (Pawlowska and Brenguier, 2000). They showed that a 15% increase of cloud depth can have the same effect for cloud albedo as a doubling of the cloud droplet number concentration (CDNC). In literature a common approach to derive these two quantities from satellites is a model which assumes an adiabatically increasing liquid water content, the so-called adiabatic model (e.g. Boers et al, 2006, Bennartz et al., 2007, Min et al., 2012). Nonadiabatic liquid water content (LWC) profiles can be either attributed to vertical variations of CDNC or reff due to inhomogeneous and homogeneous mixing, respectively (Boers et al., 2006). In Boers et al. (1998) and Pawlowska and Brenguier (2000) inhomogeneous mixing is seen as the main cause for deviations from the theoretical adiabatic profiles. Min et al. (2012) states that knowing this cloud adiabacity is a key factor to gain a more accurate retrieval of CDNC from satellites. While satellite retrieved cloud geometrical thickness can be easily compared to ground-based remote sensing, the verification of CDNC is not as straightforward possible due to a lack of in-situ measurements (Roebeling et al., 2007). In this study we apply a method to retrieve the cloud droplet number concentration with a set of ground remote sensing instruments, specifically a cloud radar, a ceilometer and a microwave radiometer. Several methods using different sets of instruments are described in the literature: e.g. radar-radiometer retrievals (Frisch, 1998, Remillard et al., 2013), Z-LWC relationships using cloud radar only (Liao and Sassen, 1996, Fox and Illingworth, 1997) or radar-lidar retrievals (Martucci and O'Dowd, 2011).

Herein, two alternative approaches to retrieve CDNC are compared. The first method is based on the theoretical relationship of radar reflectivity to the LWC profile as described in Fox and Illingworth (1997), the second one is based on an optimal estimation method (Rodgers, 2000) applying radar,

ceilometer and microwave radiometer, using satellite retrieved CDNC as a first guess.
In section 2 we describe the preparation of our dataset, followed by a description of the methods in section 3 and results in section 4. Finally we give a conclusion and outlook.

2. DATA AVAILABILITY AND PROCESSING

The LACROS (Leipzig) site comprises several ground measurement instruments: a HATPRO microwave radiometer together with a rain gauge, a 35GHz MIRA cloud radar and a CHM15X ceilometer. For the satellite perspective we use the data from MSG SEVIRI.

Ground measurements are processed with the Cloudnet algorithm package (Illingworth and Hogan, 2007). The measurements are put on a common grid of 60 m spatial resolution and 30 s time resolution. Further input data in form of numerical weather prediction model (NWP) fields is required. Here we use the COSMO-DE model. The following products from Cloudnet are used within our study: (a) the attenuation-corrected radar reflectivity and its error in terms of one standard-deviation, (b) the target classification of the atmospheric profile (fig. 1), (c) the cloud base height derived from the ceilometer as well as the cloud top height derived from the cloud radar, (d) the liquid water path (LWP) retrieved from the microwave radiometer (MWR) with the method described in Gaussiat (2007) and its error in terms of one standard-deviation. Whenever we refer to those quantities the Cloudnet quantities are meant, unless stated otherwise.

Satellite products are processed with the NWC SAF and KNMI-CPP package. The NWC SAF (www.nwcsaf.org) aims to provide operational Nowcasting and Very Short Range Forecasting products derived from satellites. The following two products are used within this study: the cloud mask (CMa), and the cloud top height (CTH). NWC SAF applies different multispectral tests using SEVIRI channels to discriminate cloudy from cloud-free pixels to derive the CMa. The CTH is achieved by simulating SEVIRI channels using the RTTOV radiative transfer model given NWP input data. For low and medium level clouds, which have a sufficient vertical extent, the CTH can be derived from a best fit of the 10.8 channel brightness temperatures. The NWC SAF CMa is used as input for the Cloud Physical Properties retrieval of the KNMI (KNMI-CPP) (msgcpp.knmi.nl). The algorithm derives the cloud optical depth τ and effective radius r_{eff} based on the method described by Nakajima and King (1990). From these two quantities we can calculate the cloud water path (CWP, liquid + ice water path) from eq. 1.

$$CWP = \frac{2}{3} \rho \tau r_{eff} \quad \text{(eq. 1)}$$

In the absence of ice clouds, this directly equals the LWP. Furthermore the CDNC can be estimated from the KNMI-CPP retrieval by assuming an adiabatic cloud profile (eq 2.).

$$N = \alpha \tau^{0.5} r_{eff}^{-2.5} \quad \text{(eq. 2)}$$

N is the CDNC, α is a factor depending on the adiabatic lapse rate of the LWC mixing ratio (Γ_{ad}).

3. METHODOLOGY

In the following we first retrieve the CDNC and subsequently the vertical profiles of reff and LWC given the ground measurements at LACROS and the retrieved products from Cloudnet. We assume that the droplet size distributions follows a Gamma shape distribution and that the CDNC is constant with height. Thereby it is assumed that no mixing or drizzle/rain processes takes place. Microphysical quantities are directly linked to n-th moments of the size distribution: CDNC is proportional to the zeroth moment, LWC is proportional to the third moment and reff is the ratio of the third and the second moment (Frisch et al., 2002).

3.1. Retrieval of cloud droplet number concentration

To retrieve the cloud droplet number concentration we combine the ground-site retrieved LWP and radar reflectivity following the relationship by Fox and Illingworth (F-I) (eq. 3).

$$Z \sim k^{-1} N^{-1} \rho^{-2} q^2 \quad \text{(eq. 3)}$$

Here k describes the relationship of volume and effective radius, ρ is the density of liquid water, N is the CDNC and q is the LWC.

Since the vertical profile of LWC is unknown we integrate eq. 3 to yield LWP Q and are able to calculate CDNC under the assumption that it is not height-dependent (eq. 4). The integral of the radar reflectivity is calculated numerically with a trapezoid rule.

$$N \sim k^{-1} \rho^{-2} Q^2 \left(\int Z(z)\, dz \right)^{-2} \quad \text{(eq. 4)}$$

3.2 Retrieval of liquid water content and effective radius profiles

An adiabatic model of the vertical distribution of LWC and reff is a common first choice for low-level liquid water clouds. Thereby it is assumed that the LWC is increasing linearly with height z (eq. 5). The effective radius is increasing with height to the power of one-third (eq. 6).

$$q(z) = f_{ad} \Gamma_{ad} z \quad \text{(eq. 5)}$$

$$r_{eff} \sim \left(f_{ad} \Gamma_{ad} z \right)^{(1/3)} \left(k N \right)^{(-1/3)} \quad \text{(eq. 6)}$$

Since clouds may depart from the pure adiabatic description an adiabatic factor f_{ad} can be used to describe the deviation of the adiabacity of the cloud LWC profile. A perfect adiabatic cloud would have an adiabatic factor of f_{ad}=1. LWP from the MWR can be used to scale the adiabatic LWC. This gives the scaled adiabatic LWC profile and the adiabatic factor.

3.3. Optimal estimation of cloud droplet number concentration and liquid water path

In the following approach we find an optimal state for CDNC and LWP in the sense that a background state and observations, both with error covariances, are optimally combined. We follow the method described by Rodgers (2000) and minimize a cost function using the Levenberg-Marquardt minimization iteration (eq. 7) (see also Hewison, 2007) with a Chi-squared test as a stop criterium.

$$x_{(i+1)} = x_{(i)} + \left((1+\gamma) B^{-1} + H_i^T R^{-1} H_i \right)^{-1} \left[H_i^T R^{-1} \left(y - H(x_{(i)}) \right) - B^{-1} \left(x_{(i)} - x_b \right) \right] \quad \text{(eq. 7)}$$

In our case the observation vector is the radar reflectivity processed by Cloudnet. The state vector includes CDNC and LWP. The background state for CDNC is the KNMI-CPP derived CDNC assuming perfect adiabatic clouds. If no satellite data is available a climatological value of 200 cm^{-3} is assumed. This value is believed to be a reasonable assumption for land areas (Zhao et al., 2012). The background LWP is the Cloudnet LWP. Although this might be seen as a measurement value in the original optimal estimation sense, for the forward model applied here it is required as an input parameter to simulate the radar reflectivity profile. Our simple forward model applies the theoretical relationship of Z to LWC and CDNC as described in F-I. Two steps are required: (1) calculating the scaled adiabatic LWC profile within the cloud borders, (2) simulating the reflectivity given background CDNC and LWC profile using the relationship from F-I. Our forward model is cheap in terms of computing time compared to a full radiative transfer model. This is important since the forward model has to be called several times for each profile optimization. The Jacobian matrix is evaluated with a brute force method by applying small changes to the state vector elements and calculating the finite differences afterwards. In the observation error covariance matrix, only the diagonal elements are nonzero. Thereby we assume that there is no correlation between the different height levels. The variances are obtained by the standard deviation values provided by Cloudnet. Within the background error covariance matrix it is assumed that there is no correlation between LWP and CDNC. The limitations of our forward model are addressed in the next section.

4. RESULTS

At the 27 September 2012 a homogeneous liquid water cloud layer without overlaying Cirrus cloud was observed. Only a very short period of drizzle is observed around 16 UTC, coinciding with the freezing of cloud droplets. This provides a good situation for a case study to compare satellite and

ground measurements and their retrievals. In Fig. 1 the time series from 9 to 18 UTC is shown. Comparing the NWC SAF CTH with the Cloudnet CTH we find rather good agreements (correlation of 85%) when the cloud layer is unbroken. According to Lagrangian perspective the time evolution can be also seen as a spatial picture. This makes it possible to compare satellite pixels of 4x6 km size to much higher resolved measurements in space and time from Cloudnet. Still, differences in the field of view from the satellite and ground perspective can introduce deviations.

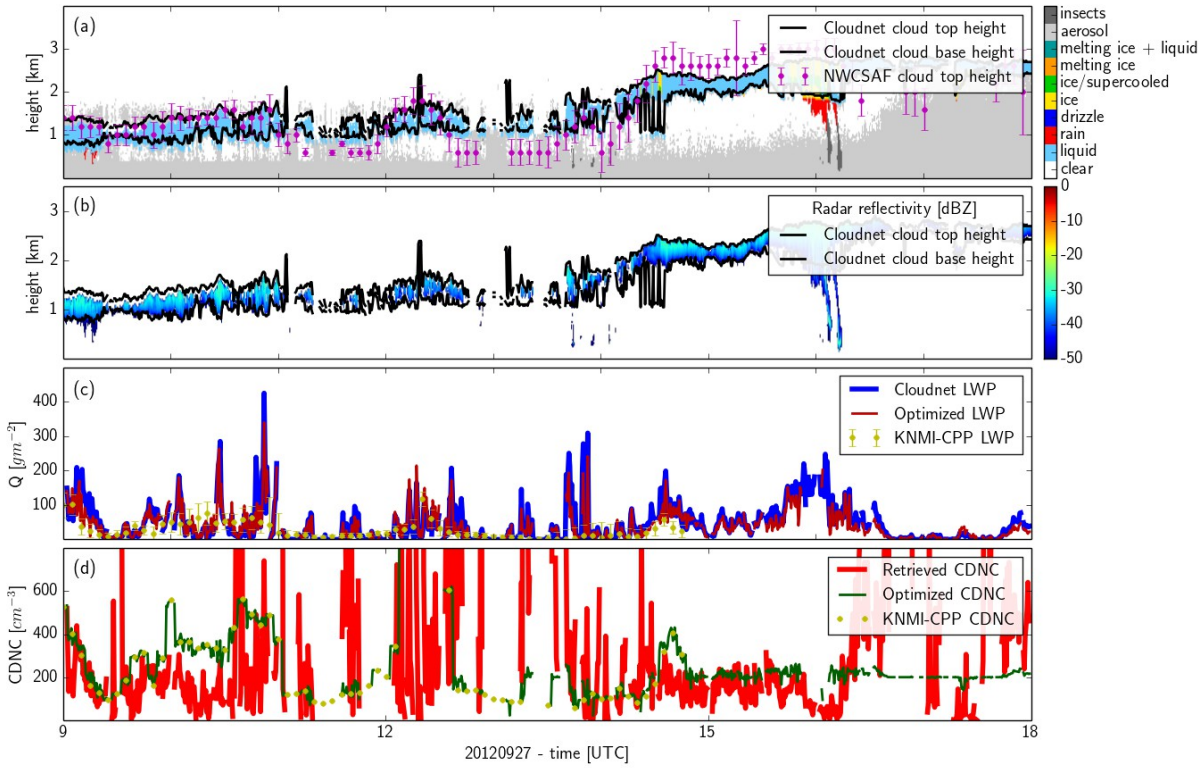

***Figure 1*: (a) Cloudnet classification and cloud borders detected by Cloudnet as well as the CTH detected from NWC SAF for the satellite pixel of the Leipzig position. Error-bars give the standard deviation in the area of +/- 3 pixel. (b) shows the radar reflectivity and Cloudnet cloud borders. (c) Cloudnet LWP (blue line), the optimized LWP (red line) and the LWP from KNMI-CPP and its standard deviation (yellow dots). (d) Retrieved CDNC as described in chapter 3.1. (red line), optimized CDNC (green line) and CDNC from KNMI-CPP (yellow dots).**

F-I-retrieved CDNC shows large variations during very short time intervals, while optimized CDNC stays more smooth during the same period. This might be attributed to some part to the background state CDNC coming from 5min resolution satellite retrievals. Since an independent source for verification is missing, it can't be verified if the jumps are a real phenomenon. However jumps within the number of cloud droplets by over 400 cm^{-3} back and forth within several seconds seem physically unrealistic. The explanation for these jumps might rather be attributed to invalid assumptions within the retrieval for these time periods.

The optimization method applied here still has some issues that have to be addressed. The forward model might not be able to represent the measured radar profile in case of a wrong detection of the cloud base height or larger deviations from the linear LWC profile (mixing processes). The method seems to work quite well when the profile within the cloud follows a theoretical (sub-)adiabatic vertical profile as in fig. 2. Due to the minimum radar detection limit ($Z \sim r^6$) the lowest part of the cloud might not be detected, while the ceilometer has a better possibility to detect the actual cloud base. This can result in biased outcomes of the optimization process, where we try to find an optimal state by including the measured radar profile.

Taking a look at the adiabatic factor f_{ad} that is derived from the scaling of the theoretical adiabatic LWC profile with the optimized LWP as described in section 3.2, it can be seen that the median is 0.4 with a standard deviation of 0.2, and therefore the clouds here show sub-adiabatic properties. This can also

be seen by taking a look at actual profiles. Two example profiles are given in fig. 2. The theoretical adiabatic curves give a much larger integrated LWC than the LWP measured with the MWR.

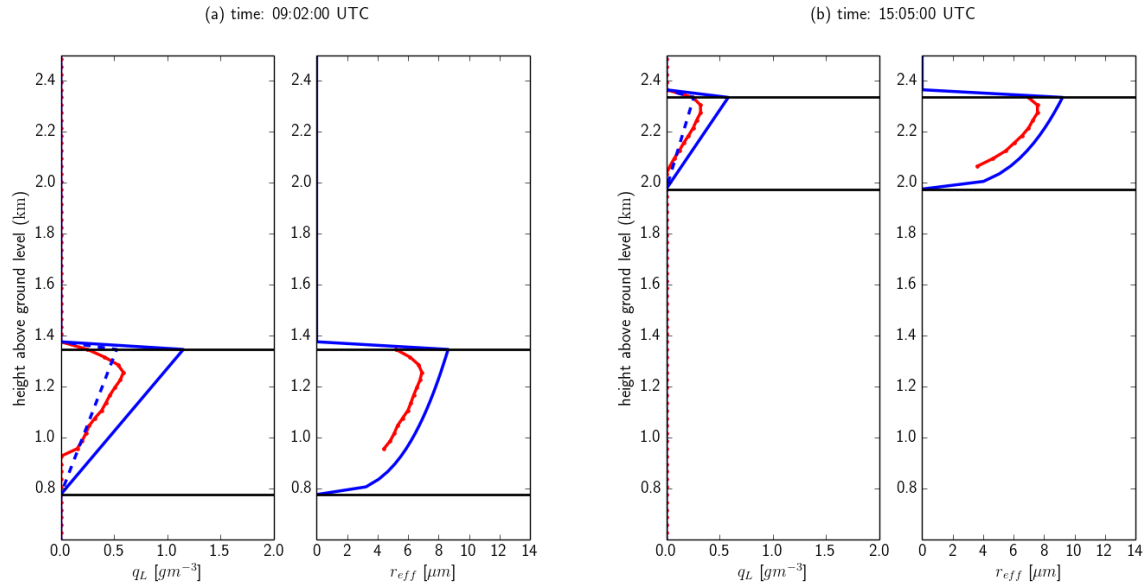

***Figure 2*: Two cloud profiles of LWC and reff. Blue solid lines represent the profiles calculated with the theoretical adiabatic model. Blue dashed lines represent the scaled adiabatic profiles. Red lines represent the profiles derived from the F-I method using optimized CDNC.**

5. CONCLUSION AND OUTLOOK

Key quantities for the investigation of the first indirect aerosol effect are the geometrical cloud depth and the cloud droplet number concentration. To derive both from satellite an adiabatic assumption about the cloud vertical profile is required. We tried to derive information about these two quantities combining satellite and ground measurements for one case study with a homogenous one-layer liquid water cloud. We apply a radar-radiometer retrieval and an optimal estimation method for the cloud droplet number concentration. The optimal estimation method shows a more smooth time series. It was observed that for our case study the profiles are sub-adiabatic on average.
For the optimal estimation a more complex forward model (e.g. radiative transfer simulations) may be beneficial to account for complex processes like mixing. Also the error statistics at the moment don't consider covariances, which might not be a realistic assumption especially for the neighboring levels of the radar reflectivity profile.
Investigations of longer time-series at different locations will be helpful to learn about the adiabacity of the clouds, which has turned out of being a key factor for investigations of the first indirect aerosol effect.

REFERENCES

Bennartz, R., (2007) Global assessment of marine boundary later cloud droplet number concentration from satellite, J. Geophys. Res., **112**, D02201, doi:10.1029/2006JD007547.

Boers, R., Acarreta, J. A., and Gras, J. L., (2006) Satellite monitoring of the first indirect aerosol effect: Retrieval of the droplet concentration of water clouds, J. Geophys. Res., **111**, D22208, doi:10.1029/2005JD006838.

Brenguier, J.-L., Pawlowska, H., Schüller, L., Preusker, R., Fischer, J., and Fouquart, Y.: Radiative properties of boundary layer clouds: Droplet effective radius versus number concentration, J. Atmos. Sci., **57**, 6, pp 803–821.

Derrien, M. and Le Gléau, H., (2003) SAFNWC/MSG SEVIRI cloud products, Proc. The 2002 EUMETSAT Meteorological Satellite Conference, Weimar, Germany, **191**, pp 198

Fox, N. I. and Illingworth, A. J., (1997) The retrieval of stratocumulus cloud properties by ground-based cloud RADAR, J. Appl. Meteorol., **36**, 5, pp 485–492.

Frisch, A. S., Feingold, G., Fairall, C. W., Uttal, T., and Snider, J. B., (1998) On cloud RADAR and microwave radiometer measurements of stratus cloud liquid water profiles, J. Geophys. Res., **103**, D18, pp 195-197.

Frisch, A. S., Shupe, M., Djalalova, I., Feingold, G. and Poellot, M., (2002) The Retrieval of Stratus Cloud Droplet Effective Radius with Cloud Radars, J. Atmos. Ocean. Tech., **19**, 6, pp 835-842.

Gaussiat, N., Hogan, R. J., Illingworth, A. J., (2007) Accurate Liquid Water Path Retrieval from Low-Cost Microwave Radiometers Using Additional Information from a Lidar Ceilometer and Operational Forecast Models, J. Atmos. Ocean. Tech., **24**, 9, pp 1562-1575.

Hewison, T. J., (2007) 1D-VAR Retrieval of Temperature and Humidity Profiles From a Ground-Based Microwave Radiometer, IEEE Trans. Geos. Rem. Sens., **45**, 7, pp 2163-2168.

Illingworth, A. J., Hogan, R. J., O'Connor, E. J., Bouniol, D., Brooks, M. E., Delanoe, J., Donovan, D. P., Gaussiat, N., Goddard, J. W. F., Haeffelin, M., Klein Baltink, H., Krasnov, O. A., Pelon, J., Piriou, J. M., and van Zadelhoff, G. J., (2007) Cloudnet – continuous evaluation of cloud profiles in seven operational models using ground-based observations, B. Am. Meteorol. Soc., **88**, 6, pp 883–898.

Sassen, K. and Liao, L., (1996) Estimation of Cloud Content by W-Band Radar, J. Appl. Met., **35**, 6, pp 932-938.

Martucci, G. and O'Dowd, C. D., (2011) Ground-based retrieval of continental and marine warm cloud microphysics, Atm. Meas. Tech., **4**, 12, pp 2749-2765

Min, Q., Joseph, E., Lin, Y., Min, L., Yin, B., Daum, P. H., Kleinman, L. I., Wang, J. and Lee, Y.-N., (2012) Comparison of MODIS cloud microphysical properties with in-situ measurements over the Southeast Pacific, **12**, 23, pp 11261-11273

Nakajima, T., and M. D. King, (1990) Determination of the optical thickness and effective radius of clouds from reflected solar radiation measurements: part I., Theory, J. Atmos. Sci., **47**, 15, pp 1878–1893.

Twomey, S., (1977) The influence of pollution on the shortwave albedo of clouds. J. Atmos. Sci., **34**, 7, pp 1149–1152.

Rémillard, J., Kollias, P. and Szyrmer, W., (2013) Radar-radiometer retrievals of cloud number concentration and dispersion parameter in nondrizzling marine stratocumulus, Atm. Meas. Tech., **6**, 7, pp 1817-1828

Roebeling, R. A., Placidi, S., Donovan, D. P., Russchenberg, H. W. J., Feijt, A. J, (2008) Validation of liquid cloud property retrievals from SEVIRI using ground-based observations, Geo. Res. L., **35**, 5, L05814

Rodgers, C. D., (2000) Inverse Methods for Atmospheric Sounding: Theory and Practice, World Sci., River Edge, N. J..

Zhao, C., Xie, S., Klein, S. A., Stephan A., Protat, A., Shupe, M. D., McFarlane, S. A., Comstock, J. M., Delanoe, J., Deng, M., Dunn, M. and others, (2012) Toward understanding of differences in current cloud retrievals of ARM ground-based measurements, J. Geop. Res., **117**, D10, pp 1984-2012.